RSC Advances

PAPER

View Article Online
View Journal | View Issue

Cite this: *RSC Adv.*, 2015, **5**, 50137

Novel donor–acceptor polymers based on 7-perfluorophenyl-6*H*-[1,2,5]thiadiazole[3,4-*g*]-benzoimidazole for bulk heterojunction solar cells

Benlin Hu,†[a] Miaomiao Li,†[b] Wangqiao Chen,[a] Xiangjian Wan,[b] Yongsheng Chen*[b] and Qichun Zhang*[ac]

Received 2nd April 2015
Accepted 1st June 2015

DOI: 10.1039/c5ra05849j

www.rsc.org/advances

Three new fluorinated D–A type conjugated polymers based on a novel building unit 7-perfluorophenyl-6*H*-[1,2,5]thiadiazole[3,4-*g*]benzoimidazole have been synthesized through a Sitlle coupling reaction. The as-prepared polymers exhibit a narrow band gap (from 1.31 to 1.34 eV) and low lying energy levels with lowest occupied molecular orbital (LUMO) energy levels of −3.95, −3.97 and −4.15 eV, respectively. These polymers exhibit excellent solubility in common organic solvents due to the introduction of perfluorophenyl and long alkyl sidechains. The power conversion efficiency (PCE) of solar cells based on these as-prepared polymers and $PC_{71}BM$ could reach as high as 1.92%. Our results could provide a simple strategy for designing high performance D–A polymers based on this unit and a potential to further improve their performance.

Introduction

Since the conception of bulk-heterojunction (BHJ) was proposed in 1992, BHJ solar cells have attracted numerous attentions in the past two decades.[1–8] Especially, the power conversion efficiencies (PCEs) of BHJ solar cells based on polymer/fullerene blends are approaching 10% for single-junction cells, which can be attributed to the rapid progress of novel donor–acceptor (D–A) polymers.[9–19] The most charming feature of D–A polymers for BHJ solar cells is the high flexibility in tuning the absorption and frontier molecular orbital energy levels of the objective D–A polymers. Generally, the highest occupied molecular orbital (HOMO) and the lowest occupied molecular orbital (LUMO) energy levels of D–A polymers can be estimated *via* the HOMO level of the "donor" (D) structural unit and the LUMO level of the "acceptor" (A) unit, respectively. This important feature enables scientists to design and synthesize new polymers with a suitable LUMO level through using specialized acceptors and in coupling with a low bandgap to obtain a high open circuit voltage (V_{oc}) and a high short circuit current (J_{sc}), simultaneously.[17–20] Besides that the aromatic units in D–A polymers can largely determine the photovoltaic performance of the BHJ solar cells, other structural parameters including the peripheral side chains and functional substituents can also have strong influence.[12–24] Under these empirical rules, elaborate design of donors and acceptors can help maintain the upward trend of the device efficiency towards the predicted PCE of 15% for BHJ polymer solar cells.[17,25,26]

Fused aromatics, typically *via* the annulation of different small aromatic units (*e.g.*, benzene, thiophene, pyrrole, pyridine, *etc.*), are the most frequently used structural units as donors or acceptors in the D–A polymers for organic electronics.[16–18,25,27,28] Among the reported fused aromatics, D–A polymers based on 2,1,3-benzothiadiazole (BT) have been found with a PCE as high as 10%.[11,13–18,29–32] Although BT is a strong electron-withdrawing unit, it is still not strong enough to pull LUMO level down to ~−4.0 eV in D–A polymer, which could have a broad bandgap, an inferior absorption spectrum, and a lower PCE of the resulted solar cells. Therefore, introducing more electron-withdrawing groups into BT units is highly desirable to further increase the PCE of solar cells. Most of recently-reported BT derivatives are summarized in Chart 1. Generally, incorporating strong electron-withdrawing units onto BT unit is the most popular strategy. For example, quinoxaline unit has been employed as an electron-withdrawing block to form BT-M1 (Chart 1) through[32–35] a simple synthesis; however, the PCE did not show too much enhancement. Then fluorine atoms were introduced into BT systems as strong electron-withdrawing groups to improve the interaction between polymers:PCBM and electrodes, and the resulted BT-M2 and BT-M3 have become the mostly used units to improve the PCE.[21–24] In order to further increase the electron-withdrawing ability of BT unit, another strategy is to fuse two

[a]*School of Materials Science and Engineering, Nanyang Technological University, Singapore 639798, Singapore. E-mail: qczhang@ntu.edu.sg*

[b]*Key Laboratory for Functional Polymer Materials and Centre for Nanoscale Science and Technology, Institute of Polymer Chemistry, College of Chemistry, Nankai University, Tianjin 300071, China. E-mail: yschen99@nankai.edu.cn*

[c]*Division of Chemistry and Biological Chemistry, School of Physical and Mathematical Sciences, Nanyang Technological University, Singapore 637371, Singapore*

† B. Hu and M. Li contributed equally.

conjugated five-member-ring heterocycles onto one building unit to generate a novel exceptionally strong acceptor, which can be further employed as construction blocks to form low band gap polymers. For example, D–A polymers based on BT-M4 (X = S or Se) show longer wavelength absorptions and deeply LUMO energy levels, and the enhancing PCE.[36–38] If **M5** was used, conjugated polymers with BT-M5 have been demonstrated to show good PCE values.[39–41] However, the synthetic procedures of all the above-mentioned monomers are very long and tedious. Therefore, it is urgent to explore other novel strong acceptors, which could be incorporated into BT unit to enhance the PCE of solar cells.

Herein, we report novel D–A polymers based on 5*H*-imidazo[4,5-*f*]-2,1,3-benzothiadiazole (**IBT**) as an acceptor unit, where the imidazole unit is employed to improve the electron affinity. Obviously, **IBT** unit is a stronger acceptor than BT unit. Moreover, the N–H···F intramolecular interactions in the monomer of **PFIBT** can hinder the rotation of the adjacent thiophene ring and increase the coplanarity and conjugated region in the D–A copolymers, and these interactions can also lower the aromaticity of π-systems to give better charge transport and higher PCEs. Furthermore, another strong electron-withdrawing unit pentafluorophenyl is introduced into benzimidazole unit to further increase the electron affinity and produce a larger conjugated backbone than that of BT unit. The introduction of fluorine atoms is generally believed to improve the solubility and the adhesion to electrodes, and then lower the energy barrier between active layer and electrodes. In addition, the using of fluorine atoms in D–A polymers can also obtain high fill factor (FF), large short-circuit current density (J_{sc}) and high open-circuit voltage (V_{oc}).[21–24] In this paper, we designed and synthesized a novel monomers including 7-perfluorophenyl-6*H*-[1,2,5]thiadiazole[3,4-*g*]benzoimidazole (**PFIBT**) units. Three new D–A polymers based on **PFIBT** show good solubility, excellent absorption spectra in the range of 300–800 nm, and deeply LUMO energy levels. In addition, the BHJ solar cells with these polymers as donors have been fabricated and the performance of the as-prepared devices were carefully investigated.

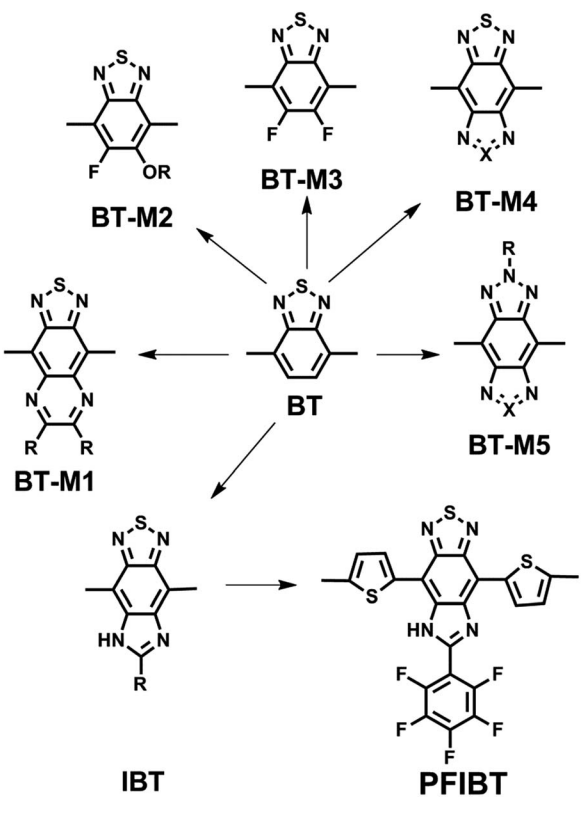

Chart 1 The chemical structures of 2,1,3-benzothiadiazole (BT) and its derivates (X = S or Se).

Experimental section

Materials and methods

Compound **1** and **M2–M4** (Scheme 1) were prepared according to the reported procedures.[12,42–47] All starting chemicals, unless otherwise specified, were purchased from Alfa Aesar or Sigma-Aldrich and used as received. [6,6]-Phenyl-C_{71}-butyric acid methyl ester ($PC_{71}BM$, >99%, EL device grade) was purchased from Solenne. All solvents were purified by normal procedure before use.

^{1}H Nuclear Magnetic Resonance (^{1}H NMR) spectra were measured at 300 MHz on a Bruker 300 AVANCE III spectrometer with chloroform ($CDCl_3$), *N*,*N*-dimethylmethanamide (DMF-d_7) or dimethyl sulfoxide (DMSO-d_6) as solvents. UV-Vis absorption spectra were recorded on a Shimadzu 2501 PC spectrophotometer at room temperature. Thermogravimetric analysis (TGA) was performed on a TA Instrument Q500 instrument under a nitrogen atmosphere with a gas-flow rate of 50 mL min^{-1} and a heating rate of 10 °C min^{-1}. Gel permeation chromatography (GPC) traces of the samples were monitored on an Agilent 1260 GPC-MDS system fitted with differential refractive index (DRI) and Ultraviolet (UV) detectors using THF as the eluent and linear polystyrenes as the molecular weight standards. Cyclic voltammetry (CV) measurements were carried out with a CHI 604E Electrochemical Workstation (CH Instruments, Shanghai Chenhua Instrument Corporation, China) under an argon atmosphere. The polymer film coated on a Pt plate (working electrode) was scanned at 10 mV s^{-1} in an anhydrous dichloromethane solution of tetrabutylammonium hexafluorophosphate (n-Bu_4NPF_6, 0.1 M), with a Pt wire and platinum gauze as the reference and counter electrodes, respectively. The thickness of the polymer film was measured by a KLA Tencor Alpha-Step Surface Profiler.

Fabrication and characterization of polymer BHJs

The devices were fabricated with a structure of glass/ITO/PEDOT:PSS/donor:acceptor/PFN/Al. The indium tin oxide coated glass substrates were cleaned sequentially with detergent, DI water, acetone, and isopropyl alcohol and then dried by a nitrogen flow. Before use, the substrate was treated with oxygen plasma. A thin layer of poly(3,4-ethylenedioxthiophene):poly(styrene sulfonate) (PEDOT:PSS) (Baytron P VP AI 4083, filtered at 0.45 μm) was spin-coated (3000 rpm, *ca.* 40 nm thick) onto ITO surface. After being baked at 150 °C for 20 min, the substrates were transferred

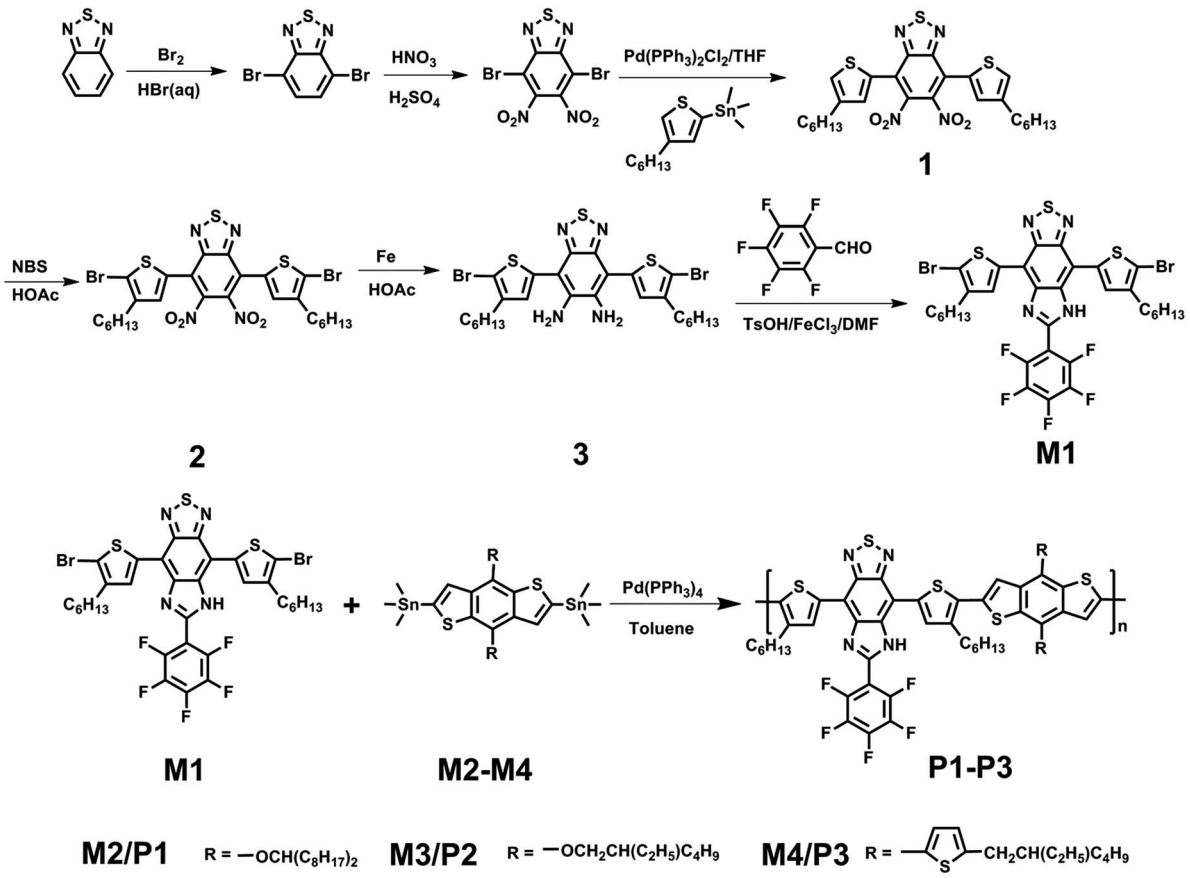

Scheme 1 The synthesis of monomer and polymers.

into an argon-filled glove box. The active layers were prepared by dissolving polymers and $PC_{71}BM$ at weight ratios of 1 : 1 (*w*/*w*) with a total concentration (20 mg mL^{-1}) in chlorobenzene, and then an active layer was deposited by spin-coating from the solution at a speed of 1500 rpm onto the ITO/PETDOT:PSS substrates for 40 s. The thickness of each active layer was ~90–100 nm. Finally, a thin layer of PFN were spin-casted on top of active layers and then Al (80 nm) was evaporated to form the top electrode. The effective area of each cell was 4 mm^2 defined by shallow masks. The current density–voltage (*J*–*V*) curves of photovoltaic devices were obtained by a Keithley 2400 source-measure unit. The devices were measured under AM 1.5 radiation (100 mW cm^{-2}) using an Oriel 96000 solar simulator. The spectral mismatch factor was calculated by comparison of the solar simulator spectrum and the AM 1.5 spectrum at room temperature. External quantum efficiency (EQE) values of the encapsulated devices were measured using a lock-in amplifier (SR810, Stanford Research Systems). The devices were illuminated by monochromatic light from a 150 W xenon lamp passing through an optical chopper and a monochromatic. Photon flux was determined by a calibrated standard silicon photodiode.

Synthesis

4,7-Bis(5-bromo-4-hexylthiophen-2-yl)-5,6-dinitro-benzo[1,2,5]-thiadiazole (**2**). Compound **1** (1.12 g, 2 mmol), was dissolved in 30 mL DMF. The resulted solution was heated to 60 °C, and *N*-bromosuccinimide (1.60 g, 9 mmol) was added to the solution in one portion. The mixture was kept at 60 °C for about 12 h until TLC analysis showed no starting material. Then, the mixture cooled to room temperature and was acidified with 2 M HCl solution (300 mL). The as-obtained solution was extracted with ethyl ether for three times. The organic layers were combined and dried Na_2SO_4, and then all solvents were evaporated. The as-resulted mixture was treated with 30 mL hexane and frozen at −15 °C for two days. Orange red crystals were collected, washed with methanol, and dried under a vacuum in a yield of 90% (1.29 g). ^1H NMR (300 MHz, $CDCl_3$): δ (ppm) d 7.17 (s, 2H), 2.62 (t, 4H, $J = 7.2$ Hz), 1.65–1.55 (m, 4H), 1.37–1.25 (m, 12H), 0.90 (t, 6H, $J = 6.9$ Hz). ^{13}C NMR (75 MHz, $CDCl_3$): δ (ppm), 151.76, 143.42, 138.29, 131.63, 129.09, 120.37, 116.88, 31.56, 29.47, 29.43, 28.75, 22.57, 14.06.

4,7-Bis(5-bromo-4-hexylthiophen-2-yl)-benzo[1,2,5]thiadiazole-5,6-diamine (**3**). Fine iron powder (0.56 g) was added to a stirred solution of 4,7-bis-(5-bromo-4-hexylthiophen-2-yl)-5,6-dinitro-benzo[1,2,5]thiadiazole (0.72 g, 1 mmol) in acetic acid (25 mL). The mixture was heated to 80 °C, stirred for 4 h and then cooled to room temperature. The cooled reaction mixture was poured carefully into 2 N NaOH aqueous solution at 0 °C. The aqueous solution was extracted with diethyl ether three times (3 × 50 mL). The combined organic solution was washed with brine, dried over anhydrous Na_2SO_4 and then evaporated to give a dark brown shiny stuff. Hexane (20 mL) was added into this shiny stuff and

kept to refrigerator two days. A reddish powder was obtained after dried under vacuum to afford compound **3** (0.59 g, 90%). ^{1}H NMR (300 MHz, $CDCl_3$): δ (ppm) 7.05 (s, 2H), 4.40 (s, 4H), 2.64 (t, 4H, $J = 7.5$ Hz), 1.70–1.60 (m, 4H), 1.42–1.25 (m, 12H), 0.90 (t, $J = 6.9$ Hz). ^{13}C NMR (75 MHz, $CDCl_3$): δ (ppm), 150.44, 142.38, 139.24, 134.79, 129.59, 110.83, 106.87, 31.62, 29.71, 29.69, 29.03, 22.60, 14.09.

4,10-Bis(5-bromo-4-hexylthiophene-2-yl)-7-(2,3,4,5,6-pentafluorophenyl)-6*H*-[1,2,5]thiadiazole[3,4-*g*]benzoimidazole (**M1**). 2,3,4,5,6-Pentafluorobenzaldehyde (196 mg, 1 mmol) and compound **3** (410 mg, 0.63 mmol) were thoroughly mixed in DMF (10 mL), and *p*-methylbenzenesulfonic acid (100 mg) was added to the solution, and the mixture was stirred overnight. Then $FeCl_3 \cdot 6H_2O$ (500 mg) was added in to the solution, and this mixture was heated to 80 °C for 3 h. After the solution cooled to room temperature, the reaction mixture was poured into water and extracted with EtOAc (3 × 50 mL), and then washed with brine (3 × 50 mL). After dried by $MgSO_4$, the organic solvent was evaporated under reduced pressure. The crude product was purified by column chromatography (eluent: DCM/hexane = 1 : 3) to yield **M1** as a purple solid (0.45 g, 85%). ^{1}H NMR (300 MHz, $CDCl_3$): δ (ppm) 9.43 (s, 1H), 8.44 (s, 1H), 7.41 (s, 1H), 2.65–2.53 (m, 4H), 1.71–1.64 (m, 4H), 1.40–1.26 (m, 12H), 0.95–0.89 (m, 6H). ^{19}F NMR (282 MHz, $CDCl_3$): δ (ppm) −137.25 (d, 2F, $J = 19.46$ Hz), −148.10 (t, 1F, $J = 21.7$ Hz), −159.35 (dd, 2F, $J = 21.1$ Hz, 20.8 Hz).

General procedure of copolymerization by Stille coupling

The equimolecular amount of **M1** and **M2–M4**, and $Pd(PPh_3)_4$ (~1.6 mol%) were dissolved in anhydrous toluene under argon. Argon was bubbled through the solution for 30 min and then the mixture was vigorously stirred at 110 °C under an argon atmosphere for 48 hours. After cooling to room temperature, the mixture was poured into methanol. After washed with methanol, oligomers and catalyst residues were removed by hexane through a Soxhlet apparatus for 24 hours.

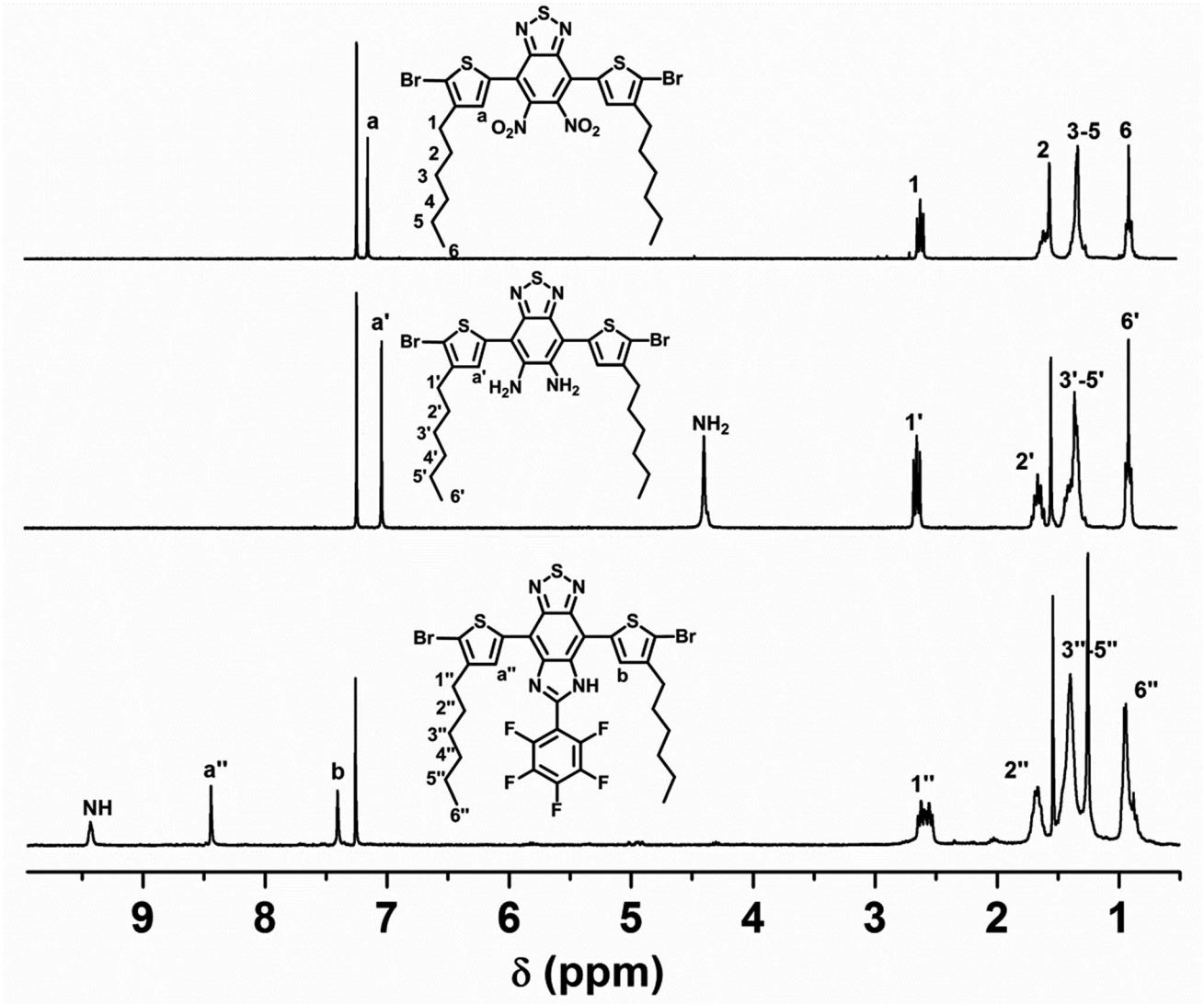

Fig. 1 The ^{1}H NMR of compound 2 (top), 3 (middle) and M1 (bottom) in $CDCl_3$.

Then, the product was extracted, by tetrahydrofuran (THF) for another 24 hours. The THF extract was concentrated and the product was precipitated by methanol, and collected by filtration and dried in vacuum overnight.

P1. M1 (208.2 mg, 0.25 mmol), **M2** (256.2 mg, 0.25 mmol), $Pd(PPh_3)_4$ (4.5 mg), toluene (3 mL). Black powder, 200 mg, yield 58%. ^{1}H NMR (300 MHz, $CDCl_3$): δ (ppm): 10.38 (s), 9.08 (s), 8.10–8.01 (m), 7.66–7.60 (m), 7.47 (d), 6.90 (s), 3.07 (s), 2.80–2.75 (m), 2.17 (s), 1.86–1.74 (m), 1.25 (br), 0.91–0.82 (m).

P2. M1 (208.2 mg, 0.25 mmol), **M3** (193.0 mg, 0.25 mmol), $Pd(PPh_3)_4$ (4.4 mg), toluene (3 mL). Black powder, 208 mg, yield 67%. ^{1}H NMR (300 MHz, $CDCl_3$): δ (ppm): 10.27 (s), 9.06 (s), 8.12–8.03 (m), 7.68–7.60 (m), 7.43 (d), 6.90 (s), 3.03 (s), 2.80–2.71 (m), 2.16 (s), 1.89–1.72 (m), 1.25 (br), 0.91–0.88 (m).

P3. M1 (208.2 mg, 0.25 mmol), **M4** (226.1 mg, 0.25 mmol), $Pd(PPh_3)_4$ (4.7 mg), toluene (3 mL). Black powder, 210 mg, yield 66.4%. ^{1}H NMR (300 MHz, $CDCl_3$): δ (ppm): 10.28 (s), 9.01–8.83 (m), 8.06–7.14 (m), 6.94 (d), 3.79 (t), 2.92–2.59 (m), 1.86–1.27 (m), 0.94 (t).

Results and discussion

Synthesis of monomers and polymers

Scheme 1 shows the synthetic routes that were used to prepare the monomer **M1** and the polymers **P1–P3**. Compound **1** was synthesized according to literature.[6,36–38] After treated with NBS, compound **1** was converted into 4,7-bis(5-bromo-4-hexylthiophen-2-yl)-5,6-dinitro-benzo[1,2,5]thiadiazole (**2**), which was further reduced by iron to form 4,7-bis(5-bromo-4-hexylthiophen-2-yl)-benzo[1,2,5]thiadiazole-5,6-diamine (**3**). Subsequently, **M1** was prepared through the condensation reaction between **3** and 2,3,4,5,6-pentafluorobenzaldehyde using methylbenzenesulfonic acid and $FeCl_3 \cdot 6H_2O$ as catalysts and air as an oxidation reagent. Fig. 1 shows the ^{1}H NMR spectra of compound **2**, **3** and **M1**. The protons on the thiophene group in compound **1** show a single peak with a chemical shift of 7.17 ppm, while the corresponding peak in compound **2** shows a little shift (0.12 ppm) to high field. The peak of amino groups in compound **2** shows a broad peak at 4.40 ppm. Because of the asymmetry from the benzimidazole group in **M1**, two different peaks of the protons on the thiophene are observed at 7.40 and 8.44 ppm; and the proton of benzimidazole ring is observed at 9.43. In addition, the chemical structure of **M1** can also be confirmed by ^{19}F NMR with three group peaks at −137.25, −148.10 and −159.35 ppm. D–A polymers **P1–P3** were synthesized through Stille coupling polymerization between **M1** and **M2–M4**. The chemical structures of all as-obtained polymers can be confirmed by ^{1}H NMR spectroscopy. Table 1 lists molecular weights and thermal decomposition temperature of **P1–P3**. The molecular weight and polydispersity index (PDI) were characterized by GPC with calibration against polystyrene standards and THF as an eluant. The number average molecular weights (M_n) of **P1–P3** were found to be 14.1, 14.3 and 16.5 kDa, with PDIs of 1.76, 1.64 and 1.85, respectively. The polymers show good thermal stability (see Fig. 2), as evidenced by its 10% weight-loss temperature ($T_{d10\%}$). **P1–P3** show good solubility in common organic solvents such as THF, chloroform and DMF.

Table 1 Molecular weights and thermal properties of P1–P3

	M_n/kDa	M_w/kDa	PDI	$T_{d10\%}$/°C
P1	14.1	24.8	1.76	309
P2	14.3	23.4	1.64	360
P3	16.5	30.3	1.85	461

Optical and electrochemical properties

The absorption spectra of all polymers in dilute THF solution (1×10^{-5} M of each repeat unit) and as solid films on glass are shown in Fig. 3, and the data are summarized in Table 2. Two main absorption bands at 300–490 nm and 510–800 nm are observed in THF solution of **P1–P3**. The bands in the range of 300–490 nm can be attributed to the π–π* transition delocalized along the π-electronic system, whereas the bands in the range of 510–800 nm can be attributed to the strong charge transfer between **IBT** acceptors and **BDT** donors. Generally, the THF solutions of **P1–P3** have strong absorptions in the whole range of 300–800 nm, even at the gap of ~500 nm. Compared with the absorption in solution, the absorption peaks of **P1–P3** thin films are red-shifted, especially the bands from the charge transfer between donors and acceptors shifted from ~600 nm to ~680 nm, suggesting stronger intermolecular interactions and aggregation in solid states than those in solution. In addition, the polymer films show no obvious absorption edge to ~1300 nm. The optical band gaps of **P1–P3**, calculated form the absorption edge in THF solution, are 1.31–1.34 eV. The polymer films show exceptional absorption in the range of 300–900 nm, indicating that the polymers may be good candidates for solar cell applications.

Electrochemical properties

Cyclic voltammetry (CV) was used to investigate the redox behaviour of all polymers and to estimate their HOMO and

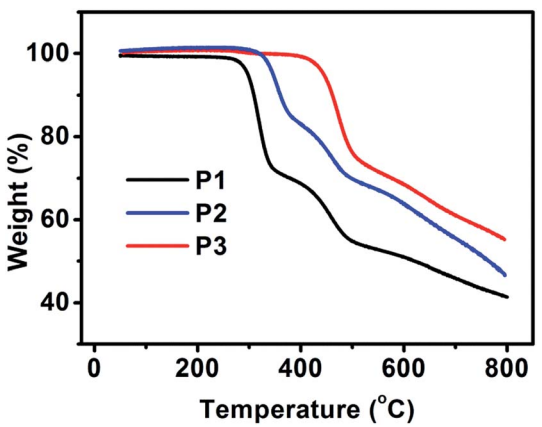

Fig. 2 TGA curves of P1–P3 under argon atmosphere at a heating rate of 10 °C min^{-1}.

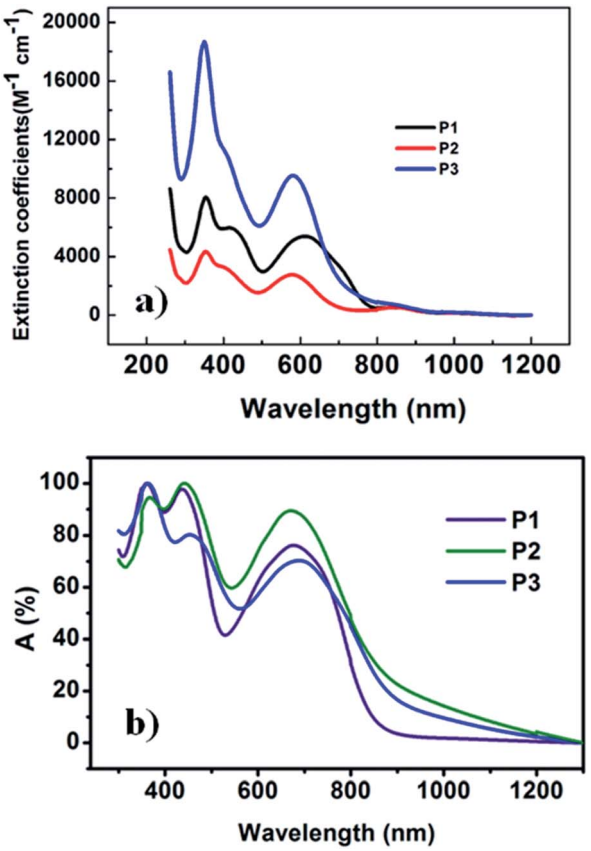

Fig. 3 UV-Vis spectra of 6F-BAHP-PC PI in THF solution (a) and films (b).

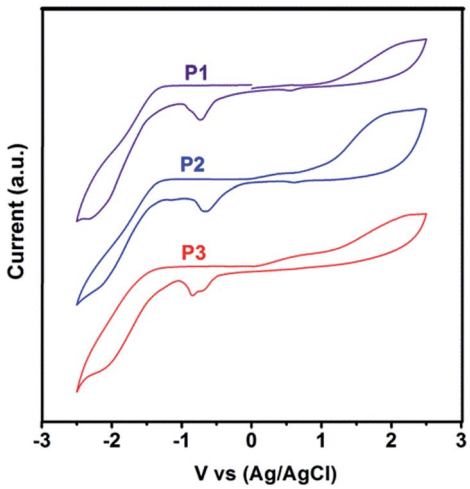

Fig. 4 Cyclic voltammograms of **P1–P3** films coated on ITO glasses.

Table 3 PSC characteristics of the polymers:PCBM BHJ PSCs

Polymers	V_{oc} (V)	J_{sc} (mA cm^{-2})	FF (%)	PCE (%)
P1	0.74	2.52	36.0	0.82
P2	0.75	4.97	36.5	1.35
P3	0.76	6.76	38.6	1.92

LUMO energy levels. The CV curves of **P1–P3** in dichloromethane using a 0.1 M solution of tetrabutylammonium tetrafluoroborate (TBATFB) at 10 mV s^{-1} are shown in Fig. 4, and the CV data are summarized in Table 3. All the polymers show obvious reduction peaks at −0.74, −0.66 and −0.84 V for **P1–P3**, respectively, which are resulted from the strong electron-withdrawing acceptor of **IBT** unit. And the corresponding reduction onsets were located at −0.51, −0.29 and −0.53 V, respectively. Polymers **P1–P3** show gradual oxidation peaks and the responding oxidation onsets were observed at 1.21, 1.04 and 1.24 V, respectively. The HOMO and LUMO levels of **P1–P3** can be calculated from the oxidation and reduction onset according to the energy level of the ferrocene reference (−4.8 eV *versus* vacuum level). The deep HOMO levels of these polymers suggest that they can transport holes. These results suggest that these polymers have great potential for the application in solar cells.

Photovoltaic properties

BHJ photovoltaic devices with **P1–P3** as donor materials and $PC_{71}BM$ as an acceptor material have been fabricated with a typical configuration of ITO/PEDOT:PSS/polymers:$PC_{71}BM$/PFN/Al. The weight ratio of polymers *vs.* $PCBM_{71}$ (1 : 1) with a total concentration of 20 mg mL^{-1} in chlorobenzene solution was employed to fabricate the devices, and the thickness of the BHJ blend was about ~90 nm. As expected, relatively high V_{oc} in the range of 0.74–0.76 V were observed in all the three polymer:PCBM based BHJ solar cells, consistent with the low-lying HOMO energy levels of **P1–P3**. The J_{sc} values for **P1–P3** are 2.52, 4.97 and 6.76 mA cm^{-2}, respectively. The corresponding PCEs of devices based on **P1–P3** are 0.82%, 1.35% and 1.92%, respectively. The external quantum efficiency (EQE) spectra of the devices with **P1–P3** are shown in Fig. 5b. From the EQE spectra, these polymers-based devices exhibit very broad photo-

Table 2 Optical and electrochemical properties of polymers **P1–P3**

	λ_{max} (nm) solution	λ_{max} (nm) film	E_g^{opta} (eV)	E_{onset}^{Ox} (V)	E_{onset}^{Red} (V)	HOMO (eV)	LUMO (eV)	E_g^{ecb} (eV)
P1	352, 615	360, 437, 671	932	1.21	−0.51	−5.69	−3.97	1.33
P2	352, 576	366, 441, 677	942	1.04	−0.29	−5.52	−4.19	1.31
P3	352, 580	363, 454, 689	925	1.24	−0.53	−5.72	−3.95	1.34

[a] Calculated from the edge of the absorption spectrum of the film. [b] E_g^{ec} = HOMO–LUMO.

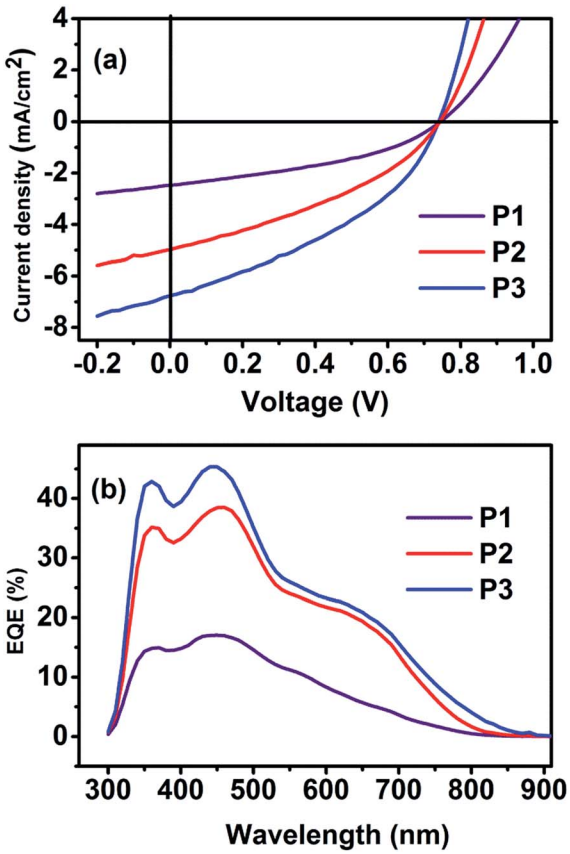

Fig. 5 (a) Current density–voltage characteristics of illuminated (AM 1.5 G, 100 mW cm^{-2}) polymer solar cells incorporating active layers of polymers/$PC_{71}BM$; (b) spectra of EQE spectra of active layers based on polymers/PCBM.

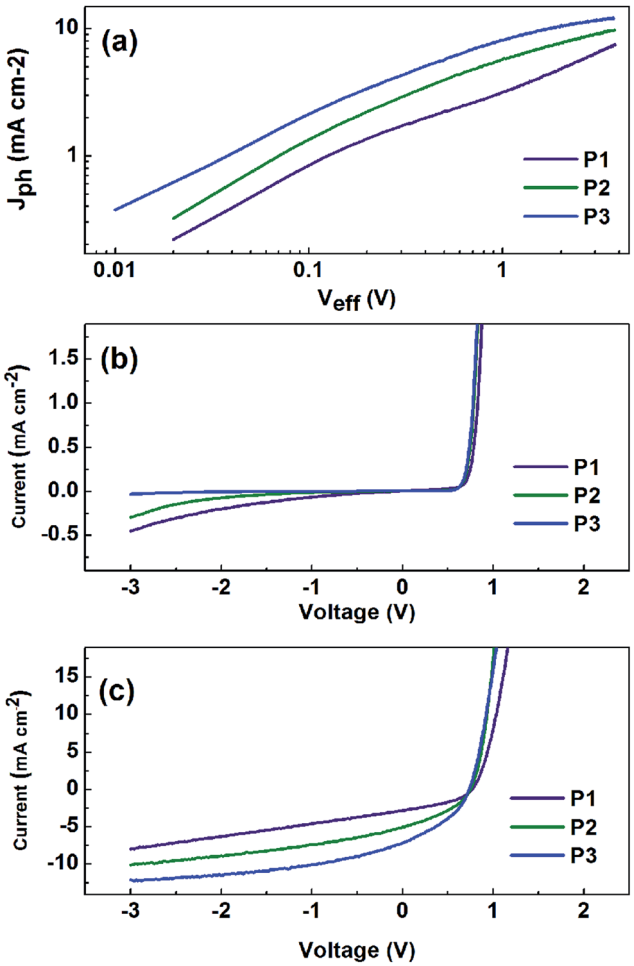

Fig. 6 (a) Photocurrent density *versus* effective voltage (J_{ph}–V_{eff}) characteristics for both devices under constant incident light intensity (AM 1.5 G, 100 mW cm^{-2}). Dark (b) and light (c) J–V to −3 V.

to-current response from 300 to about 900 nm with the highest EQE values of 17%, 38% and 45%, respectively. For the **P1**-, **P2**- and **P3**-based devices, the calculated J_{sc} obtained by the integration of the EQE curves are 2.38, 4.88 and 6.67 mA cm^{-2}, which show less 5% mismatch compared with the J_{sc} value obtained from the J–V curves.

The relationship of photocurrent density (J_{ph}) *versus* effective voltage (V_{eff}) is employed to investigate the causes of the low device performance of our devices. As shown in Fig. 6a, for **P1**–**P3** based devices, the J_{ph} shows a strong field dependence in a large bias and has not saturated even at V_{eff} = 3.8 V. This suggests the devices based on the polymers have low excition dissociation efficiency and low charge transport and collection efficiency with significant geminate and/or bimolecular recombination and/or less efficient interfacial contact, thus low FF and J_{sc}, which is attributed the poor morphology of the photoactive layers, as discussed below. The device based on **P3** show more possible tendency to be saturated than that based on **P2** and **P1**. Furthermore, light and dark current (Fig. 6b and c) are measured to confirm the origin of the poor device performance. As shown in Fig. 6c, the light current cannot be saturated even at −3 V, which suggests the collection of electrons and holes is not effective and the recombination is significant. Combining these measurements and AFM morphology study, we can conclude that the poor morphology leads generation problem and then low PCE.

Morphology study

The morphology of blend films of the polymers with fullerene derivatives plays a vital part on the charge transfer and the efficiency of bulk heterojunction solar cells. Herein, the atomic force microscopy (AFM) was applied to investigate the morphology of the polymer:$PC_{71}BM$ blend films, as shown in Fig. 7. The scan size is 5 μm × 5 μm. The root-mean-square (rms) roughness values are 6.64, 0.961 and 0.532 nm for the blend films of **P1**–**P3** with $PC_{71}BM$, respectively, which suggests that the contact between the active layer and the cathode becomes better from **P1** to **P3**. The blend films of **P1**–**P3** exhibit large phase separation and poor interpenetrating network, which is unfavourable for exciton diffusion/dissociation and charge transport. Moreover, compared with those of **P1** and **P2**, the blend film of **P3** exhibits better interpenetrating networks. As a result, the J_{sc} also becomes larger from **P1** to **P3**. Tuning

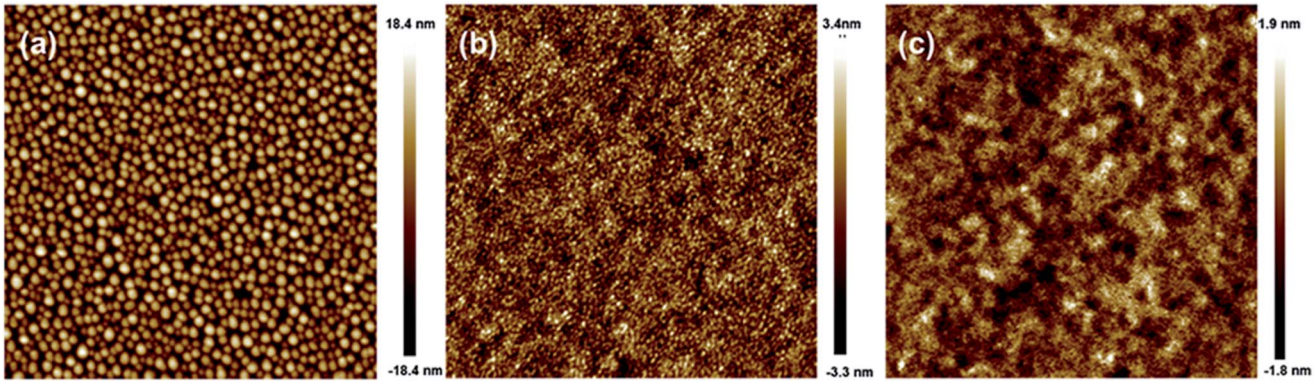

Fig. 7 AFM height images of polymers:$PC_{71}BM$, (a) **P1**, (b) **P2** and (c) **P3**. The areas are 5 μm × 5 μm.

morphology of active blend films is complex and needs further work focus on it in the future.

Acknowledgements

The authors thank Mr Kai Wang for the GPC testing. Q.Z. acknowledges the financial support AcRF Tier 1 (RG 16/12 and R/G 133/14), Tier 2 (ARC 20/12 and ARC 2/13) from MOE, and CREATE program (Nanomaterials for Energy and Water Management) from NRF Singapore.

Notes and references

1 A. J. Heeger, *Adv. Mater.*, 2014, **26**, 10.
2 N. S. Sariciftci, L. Smilowitz, A. J. Heeger and F. Wudl, *Science*, 1992, **258**, 1474.
3 (*a*) K. A. Mazzioa and C. K. Luscomebe, *Chem. Soc. Rev.*, 2015, **44**, 78; (*b*) Q. Zhang, J. Xiao, Z. Y. Yin, H. M. Duong, F. Qiao, F. Boey, X. Hu, H. Zhang and F. Wudl, *Chem.–Asian J.*, 2011, **6**, 856.
4 S. Savagatrup, A. D. Printz, T. F. O'Conor, A. V. Zaretski, D. Rodrquez, E. J. Sawyer, K. M. Rajan, R. I. Acosta, S. E Root and D. J. Lipomi, *Energy Environ. Sci.*, 2015, **8**, 55.
5 P. Wurfel, *J. Phys. C: Solid State Phys.*, 1982, **15**, 3967.
6 U. Rau, *Phys. Rev. B: Condens. Matter Mater. Phys.*, 2007, **76**, 085303.
7 J. Mattheis, J. H. Werner and U. Rau, *Phys. Rev. B: Condens. Matter Mater. Phys.*, 2008, **77**, 085203.
8 T. Kirchartz, K. Taretto and U. Rau, *J. Phys. Chem. C*, 2009, **113**, 17958.
9 (*a*) L. Dou, C.-C. Chen, K. Yoshimura, K. Ohya, W.-H. Chang, J. Gao, Y. Liu, E. Richard and Y. Yang, *Macromolecules*, 2013, **46**, 3384; (*b*) G. Sonmez, H. Meng, Q. Zhang and F. Wudl, *Adv. Funct. Mater.*, 2003, **13**, 726.
10 S. Liu, K. Zhang, J. Lu, J. Zhang, H.-L. Yip, F. Huang and Y. Cao, *J. Am. Chem. Soc.*, 2013, **135**, 15326.
11 X. Wang, P. Jiang, Y. Chen, H. Luo, Z. Zhang, H. Wang, X. Li, G. Yu and Y. Li, *Macromolecules*, 2013, **46**, 4805.
12 J. D. Yuen, R. Kumar, D. Zakhidov, J. Seifter, B. Lim, A. J. Heeger and F. Wudl, *Adv. Mater.*, 2011, **23**, 3780.
13 M. Zhang, Y. Gu, X. Guo, F. Liu, S. Zhang, L. Huo, T. P. Russell and J. Hou, *Adv. Mater.*, 2013, **25**, 4944.
14 M. Zhang, X. Guo, S. Zhang and J. Hou, *Adv. Mater.*, 2014, **26**, 1118.
15 J. Zhou, Y. Zuo, X. Wan, G. Long, Q. Zhang, W. Ni, Y. Liu, Z. Li, G. He, C. Li, B. Kan, M. Li and Y. Chen, *J. Am. Chem. Soc.*, 2013, **135**, 8484.
16 (*a*) C. Gao, L. Wang, X. Li and H. Wang, *Polym. Chem.*, 2014, **5**, 5200; (*b*) W. Chen, X. Yang, G. Long, X. Wan, Y. Chen and Q. Zhang, *J. Mater. Chem. C*, 2015, **3**, 4698.
17 T. Ameri, N. Li and C. J. Brabec, *Energy Environ. Sci.*, 2013, **6**, 2390.
18 (*a*) L. Bian, E. Zhu, J. Tang, W. Tang and F. Zhang, *Prog. Polym. Sci.*, 2012, **37**, 1292; (*b*) B. Hu, C. Wang, J. Zhang, K. Qian, W. Chen, P. S. Lee and Q. Zhang, *RSC Adv.*, 2015, **5**, 30542; (*c*) W. Chen, T. Salim, H. Fan, L. James, Y. M. Lam and Q. Zhang, *RSC Adv.*, 2014, **4**, 25291.
19 P.-L. T. Boudreault, A. Najari and M. Leclerc, *Chem. Mater.*, 2010, **23**, 456.
20 A. Facchetti, *Chem. Mater.*, 2010, **23**, 733.
21 A. C. Stuart, J. R. Tumbleston, H. Zhou, W. Li, S. Liu, H. Ade and W. You, *J. Am. Chem. Soc.*, 2013, **135**, 1806.
22 S. C. Price, A. C. Stuart, L. Yang, H. Zhou and W. You, *J. Am. Chem. Soc.*, 2011, **133**, 4625.
23 H. Zhou, L. Yang, A. C. Stuart, S. C. Price, S. Liu and W. You, *Angew. Chem., Int. Ed.*, 2011, **50**, 2995.
24 L. Fang, Y. Zhou, Y.-X. Yao, Y. Diao, W.-Y. Lee, A. L. Appleton, R. Allen, J. Reinspach, S. C. B. Mannsfeld and Z. Bao, *Chem. Mater.*, 2013, **25**, 4874.
25 M. C. Scharber and N. S. Sariciftci, *Prog. Polym. Sci.*, 2013, **38**, 1929.
26 B. Kan, Q. Zhang, M. Li, X. Wan, W. Ni, G. Long, Y. Wang, X. Yang, H. Feng and Y. Chen, *J. Am. Chem. Soc.*, 2014, **136**, 15529.
27 Y. Jiang, M. Yang, X. Huang, J. Gao, C. Zhan and S. Xiao, *Polym. Chem.*, 2015, **6**, 1383.
28 S. Shi, X. Xie, P. Jiang, S. Chen, L. Wang, M. Wang, H. Wang, X. Li, G. Yu and Y. Li, *Macromolecules*, 2013, **46**, 3358.
29 T. Lei, J.-H. Dou, Z.-J. Ma, C.-J. Liu, J.-Y. Wang and J. Pei, *Chem. Sci.*, 2013, **4**, 2447.

30 Y. Li, J. Zou, H.-L. Yip, C.-Z. Li, Y. Zhang, C.-C. Chueh, J. Intemann, Y. Xu, P.-W. Liang, Y. Chen and A. K. Y. Jen, *Macromolecules*, 2013, **46**, 5497.

31 (*a*) H.-H. Chang, C.-E. Tsai, Y.-Y. Lai, W.-W. Liang, S.-L. Hsu, C.-S. Hsu and Y.-J. Cheng, *Macromolecules*, 2013, **46**, 7715; (*b*) B. Hu, C. Wang, J. Wang, J. Gao, K. Wang, J. Wu, G. Zhang, W. Cheng, B. Venkateswarlu, M. Wang, P. S. Lee and Q. Zhang, *Chem. Sci.*, 2014, **5**, 3404–3408.

32 (*a*) C.-Y. Yu, C.-P. Chen, S.-H. Chan, G.-W. Hwang and C. Ting, *Chem. Mater.*, 2009, **21**, 3262; (*b*) W. Chen, Q. Zhang, T. Salim, S. A. Ekahana, X. Wan, T. C. Sum, Y. M. Lam, A. C. H. Huan, Y. Chen and Q. Zhang, *Tetrahedron*, 2014, **70**, 6217.

33 X. Zhang, T. T. Steckler, R. R. Dasari, S. Ohira, W. J. Potscavage, S. P. Tiwari, S. Coppee, S. Ellinger, S. Barlow, J.-L. Bredas, B. Kippelen, J. R. Reynolds and S. R. Marder, *J. Mater. Chem.*, 2010, **20**, 123.

34 V. Tamilavan, M. Song, S.-H. Jin, H. J. Park, U. C. Yoon and M. H. Hyun, *Synth. Met.*, 2012, **162**, 1184.

35 M. L. Keshtov, D. V. Marochkin, V. S. Kochurov, A. R. Khokhlov, E. N. Koukaras and G. D. Sharma, *Polym. Chem.*, 2013, **4**, 4033.

36 C. Kitamura, S. Tanaka and Y. Yamashita, *Chem. Mater.*, 1996, **8**, 570–578.

37 H. Li, T. L. Tam, Y. M. Lam, S. G. Mhaisalkar and A. C. Grimsdale, *Org. Lett.*, 2010, **13**, 46.

38 M. L. Keshtov, D. V. Marochkin, V. S. Kochurov, A. R. Khokhlov, E. N. Koukaras and G. D. Sharma, *J. Mater. Chem. A*, 2014, **2**, 155.

39 T. L. D. Tam, W. Ye, H. H. R. Tan, F. Zhou, H. Su, S. G. Mhaisalkar and A. C. Grimsdale, *J. Org. Chem.*, 2012, **77**, 10035.

40 Y. Dong, W. Cai, X. Hu, C. Zhong, F. Huang and Y. Cao, *Polymer*, 2012, **53**, 1465.

41 Y. Dong, W. Cai, M. Wang, Q. Li, L. Ying, F. Huang and Y. Cao, *Org. Electron.*, 2013, **14**, 2459.

42 E. K. Unver, S. Tarkuc, D. Baran, C. Tanyeli and L. Toppare, *Tetrahedron Lett.*, 2011, **52**, 2725.

43 J. Tong and L. An, *Asian J. Chem.*, 2013, **25**, 10460.

44 G.-Y. Chen, S.-C. Lan, P.-y. Lin, C.-W. Chu and K.-H. Wei, *J. Polym. Sci., Part A: Polym. Chem.*, 2010, **48**, 4456.

45 J. Yuan, X. Huang, H. Dong, J. Lu, T. Yang, Y. Li, A. Gallagher and W. Ma, *Org. Electron.*, 2013, **14**, 635.

46 H. Wu, B. Qu, Z. Cong, H. Liu, D. Tian, B. Gao, Z. An, C. Gao, L. Xiao, Z. Chen, H. Liu, Q. Gong and W. Wei, *React. Funct. Polym.*, 2012, **72**, 897.

47 Y. Koizumi, M. Ide, A. Saeki, C. Vijayakumar, B. Balan, M. Kawamoto and S. Seki, *Polym. Chem.*, 2013, **4**, 484.